The Canadian Mineralogist
Vol. 33, pp. 1177-1188 (1995)

MIXED-LIGAND $Cu^{2+}\Phi_6$ OCTAHEDRA IN MINERALS: OBSERVED STEREOCHEMISTRY AND HARTREE–FOCK CALCULATIONS

PETER C. BURNS[1] AND FRANK C. HAWTHORNE

Department of Geological Sciences, University of Manitoba, Winnipeg, Manitoba R3T 2N2

ABSTRACT

Examination of Cu^{2+} oxysalt mineral structures shows that many contain $Cu^{2+}\Phi_6$ mixed-ligand octahedra, with $\Phi = (O^{2-}, OH^-, H_2O)$ and 1, 2 or 4 Cl. Mixed-ligand $Cu^{2+}\Phi_6$ octahedra with 2 Cl are the most common, and there are no examples that contain 3 or 5 Cl ligands. In all cases, the octahedra are (4 + 2)-distorted owing to the Jahn–Teller effect, and the Cl ligands occur in the apical positions of the distorted octahedra wherever possible. Hartree–Fock molecular-orbital calculations for the $[Cu^{2+}(H_2O)_4(ClH)_2]^{2+}$ and $[Cu^{2+}(H_2O)_5(ClH)]^{2+}$ model clusters give Cu–(H_2O) and Cu–Cl bond-lengths consistent with those observed in minerals. These calculations predict the (4 + 2)-distortion of the $Cu^{2+}\Phi_6$ octahedra, as well as the strong preference shown by Cl ligands for the apical position of the distorted octahedron. Potential-energy surfaces calculated for each cluster are in good general agreement with the $Cu^{2+}\Phi_6$ geometries observed in minerals. These calculations have demonstrated that molecular-orbital calculations using the cluster approach are good models of local $Cu^{2+}\Phi_6$ octahedra in mineral structures.

Keywords: copper, copper oxysalt mineral, molecular-orbital calculation, Hartree–Fock, mixed-ligand octahedra, theoretical mineralogy.

SOMMAIRE

Un examen des structures des oxysels de Cu^{2+} montre que plusieurs contiennent des octaèdres $Cu^{2+}\Phi_6$ à ligands mixtes, dans lesquels Φ représente O^{2-}, OH^-, H_2O, et 1, 2 ou 4 atomes de Cl. Les groupes $Cu^{2+}\Phi_6$ à 2 Cl sont les plus répandus; aucun exemple n'est connu contenant 3 ou 5 ligands de Cl. Dans tous les cas, les octaèdres sont difformes de type (4 + 2) à cause de l'effet de Jahn–Teller, et les ligands Cl se trouvent dans les positions apicales des octaèdres difformes dans la mesure du possible. Les calculs d'orbites moléculaires selon la méthode de Hartree–Fock pour évaluer la stabilité des groupements $[Cu^{2+}(H_2O)_4(ClH)_2]^{2+}$ et $[Cu^{2+}(H_2O)_5(ClH)]^{2+}$ produisent des longueurs de liaison Cu–(H_2O) et Cu–Cl conformes aux valeurs observées dans les minéraux. Ces calculs prédisent la distorsion (4 + 2) des groupes $Cu^{2+}\Phi_6$, de même que la forte préférence des ligands Cl pour la position apicale des octaèdres difformes. Les surfaces d'énergie potentielle calculées pour chaque agencement concordent bien avec la géométrie des groupes $Cu^{2+}\Phi_6$ observée dans les minéraux. Ces résultats démontrent que les calculs d'orbites moléculaires axés sur l'évaluation des agencements $Cu^{2+}\Phi_6$ locaux produisent de bons modèles applicables aux structures des minéraux.

(Traduit par la Rédaction)

Mots-clés: cuivre, minéraux oxysels de cuivre, calcul d'orbites moléculaires, Hartree–Fock, octaèdres à ligands mixtes, minéralogie théorique.

INTRODUCTION

The Cu^{2+} oxysalt minerals generally are not isostructural with non-Cu^{2+} analogues, and as such, they have often been considered somewhat of an enigma in Mineralogy. The structural diversity shown by Cu^{2+} oxysalt minerals may, at least in part, be attributed to the large number of coordination polyhedra associated with the Cu^{2+} cation: six-coordinate octahedral, six-coordinate trigonal-prismatic, five-coordinate square-pyramidal, five-coordinate triangular-bipyramidal, and four-coordinate square-planar arrangements all occur. Of these coordination geometries, the octahedron is by far the most common.

There are about one hundred refined structures of minerals that contain $Cu^{2+}\phi_6$ (ϕ: O^{2-}, OH^-, H_2O) octahedra. The occurrence of regular $Cu^{2+}\phi_6$ octahedra in minerals, inorganic and organometallic compounds is exceedingly rare; almost all octahedra show marked distortion from holosymmetric geometry. The cause of this distortion has long been recognized; it is due to the electronic instability of the d^9 configuration of Cu^{2+} in octahedral coordination, as predicted by the Jahn–Teller theorem (Jahn & Teller 1937). Octahedral complexes with an electronic degeneracy in the e_g

---

[1] Current address: Department of Earth and Planetary Sciences, University of New Mexico, Albuquerque, New Mexico 87131-1116, U.S.A.

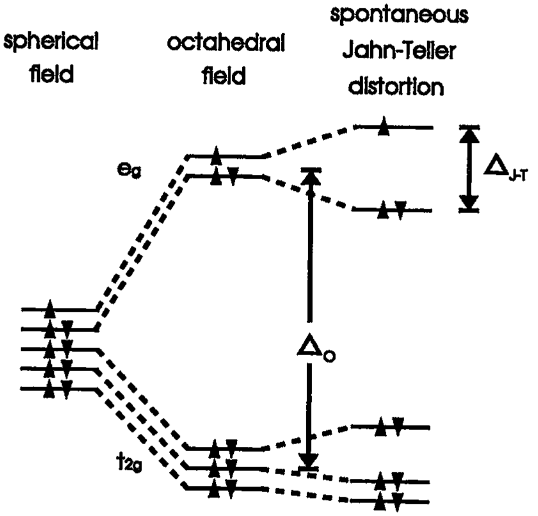

FIG. 1. The electron-energy levels for Cu^{2+} in a spherical field (left), a holosymmetric octahedral field (middle) and a distorted octahedral field (right).

orbitals, as is the case for $Cu^{2+}\phi_6$, have a single Jahn–Teller-active normal vibration mode of e_g symmetry (Deeth & Hitchman 1986). The instability is caused by vibronic couplings, but the Jahn–Teller stabilization energy ($\frac{1}{2}\Delta_{J-T}$, Fig. 1) is much greater than the energy of the e_g active vibration mode, thus an essentially stationary state occurs.

Ligand-field arguments indicate that the *d*-electron energy levels of a first-row transition-metal cation in a holosymmetric octahedral-ligand environment will be split into two groups, the triply degenerate t_{2g} orbitals (corresponding to the d_{xy}, d_{yz}, and d_{xz} atomic orbitals) and the doubly degenerate e_g orbitals (corresponding to the d_{z^2} and $d_{x^2-y^2}$ atomic orbitals) (Fig. 1). In the case of Cu^{2+}, there are nine *d* electrons, thus there is only one singly occupied *d*-orbital, and for the ground state, this will be one of the e_g orbitals. Thus, for the holosymmetric octahedron, an energetically degenerate electronic state occurs in the e_g orbitals. Arguments based on the screening of the attraction between the Cu^{2+} cation and the negatively charged ligands (Orgel 1966) indicate that either a (4 + 2)-distortion (elongation) or (2 + 4)-distortion (compression) of the octahedral-ligand geometry will lift the degeneracy, resulting in a net stabilization of the energy as predicted by the Jahn–Teller theorem (Jahn & Teller 1937). These simple screening arguments do not indicate which of the (4 + 2) or (2 + 4) distortions is favored. However, arguments have been put forward that the second-order Jahn–Teller mixing of 3*d* and 4*s* orbitals on Cu^{2+} favors the (4 + 2)-distorted arrangement (Burdett 1980, Burdett & Eisenstein 1992).

Examination of the bond lengths in the $Cu^{2+}\phi_6$ octahedra shows that virtually all are (4 + 2)-distorted (Burns 1994). Essentially, all of the $Cu–\phi_{eq}$ (equatorial) bond-lengths are in the range 1.87 to 2.12 Å, and $Cu–\phi_{ap}$ (apical) bond-lengths are in the range 2.22 to 3.12 Å. The $<Cu–\phi_{eq}>$ and $<Cu–\phi_{ap}>$ distances are 1.973 and 2.505 Å, respectively, with standard deviations of 0.048 and 0.205 Å, respectively (Burns 1994).

Numerous Cu^{2+} oxysalt minerals contain $Cu^{2+}\Phi_6$ octahedra, where Φ represents O^{2-}, OH^-, H_2O and 1, 2 or 4 Cl ligands. Owing to the mixture of ligands in these octahedra, the Cu^{2+} cation cannot achieve a holosymmetric environment, and the Jahn–Teller arguments are not strictly applicable to such polyhedra. However, a near-degenerate electronic state may occur, and distortion of the octahedron may lead to a significant net stabilization of the mixed-ligand octahedron. In $Cu^{2+}\Phi_6$ octahedra with mixed ligands, the bond-length variations are less straightforward to interpret than in the case of oxygen ligands (O^{2-}, OH^-, H_2O), as there is also an intrinsic contribution to bond-length variation that arises from the difference in size of the (O^{2-}, OH, H_2O) [$r \approx 1.36$ Å] and Cl^- [$r \approx 1.67$ Å] ligands. In this paper, we report details of mixed-ligand $Cu^{2+}\Phi_6$ octahedra in minerals in light of refined structures. Various molecular-orbital calculations were done to examine the suitability of such calculations for the description of mixed-ligand $Cu^{2+}\Phi_6$ octahedra.

Throughout this paper, the symbol ϕ refers to the set of O^{2-}, OH^- and H_2O ligands only, whereas the symbol Φ refers to the set of the O^{2-}, OH^-, H_2O and Cl ligands. A $Cu^{2+}\phi_6$ octahedron contains only (O^{2-}, OH^-, H_2O) ligands and a *mixed-ligand* $Cu^{2+}\Phi_6$ octahedron contains both (O^{2-}, OH^-, H_2O) and Cl ligands.

STRUCTURES CONTAINING $Cu^{2+}Cl_6$ OCTAHEDRA

Tolbachite, $CuCl_2$, is the only mineral known to contain $Cu^{2+}Cl_6$ octahedra (Burns & Hawthorne 1993). Crystal-structure data are available for several synthetic inorganic compounds containing $Cu^{2+}Cl_6$ octahedra (Table 1). All $Cu^{2+}Cl_6$ octahedra show (4 + 2)-distorted geometries, with $Cu–Cl_{eq}$ ranging from 2.234 to 2.381 Å (mean: 2.297 Å) and $Cu–Cl_{ap}$ ranging from 2.706 to 3.19 Å (mean: 2.918 Å). An estimate of the Cu–Cl bond-length in an undistorted $Cu^{2+}Cl_6$ octahedron may be obtained by plotting <Cu–Cl> *versus* Δ for the octahedron, where $\Delta = 1/6 \Sigma [(L_i-L_o)/L_o]^2$, L_i is any Cu–Cl distance, and L_o is the <Cu–Cl> distance for the octahedron. The intercept of the best-fit line at $\Delta = 0$ (Fig. 2) gives <Cu–Cl> = 2.43 Å for the undistorted octahedron.

MIXED-LIGAND $Cu^{2+}\Phi_6$ OCTAHEDRA IN MINERALS

In $Cu^{2+}\Phi_6$ octahedra with $\Phi = O^{2-}$, OH^-, H_2O and at least 1 Cl, a holosymmetric octahedral environment

TABLE 1. $Cu^{2+}Cl_6$ DISTANCES (Å) IN INORGANIC COMPOUNDS

	Cu-Cl$_{eq}$				Cu-Cl$_{ap}$		Ref.
$CsCu^{2+}Cl_3$	2.28	2.28	2.35	2.35	2.78	2.78	1
$Cu^{2+}Al_2Cl_8$	2.29	2.29	2.30	2.30	2.96	2.96	2
$Rb_3Cu_2^{2+}Cl_7$	2.234	2.234	2.325	2.381	2.870	2.870	3
$KCu^{2+}Cl_3$	2.248	2.267	2.314	2.322	2.941	3.113	4
$NH_4Cu^{2+}Cl_3$	2.25	2.26	2.32	2.32	2.99	3.19	4
$RbCu^{2+}Cl_3$	2.307	2.307	2.369	2.369	2.706	2.706	5
Tolbachite	2.263	2.263	2.263	2.263	2.991	2.991	6
Mean	2.297				2.918		

References: 1: Schlueter *et al.* (1966); 2: Schäfer *et al.* (1980); 3: Crama (1981b); 4: Willett *et al.* (1963); 5: Crama (1981a); 6: Burns & Hawthorne (1993).

is not possible. However, a pseudo-holosymmetric geometry is possible, such that there is a near-degenerate electronic state. In such a case, either an elongation [(4 + 2)-distortion] or a compression [(2 + 4)-distortion] of the ligand geometry will serve to remove the near-degenerate electronic state and result in a net stabilization of the octahedron.

The Cu–O and Cu–Cl bond-lengths expected for mixed-ligand $Cu^{2+}\Phi_6$ octahedra that have not been distorted by the Jahn–Teller effect may be estimated by summing the respective ionic radii. This approach gives Cu^{2+}–O^{2-} = 2.09 Å and Cu^{2+}–Cl^- = 2.40 Å [Cu^{2+} = 0.73 Å, O^{2-} = 1.36 Å (Shannon 1976); Cl^- = 1.67 Å (Whittaker & Muntus 1970)]. Independent estimates of expected <Cu^{2+}–O^{2-},OH^-,H_2O> and <Cu^{2+}–Cl^-> bond lengths for undistorted octahedra are 2.083 Å (Eby & Hawthorne 1993) and 2.43 Å, respectively, as obtained by extrapolating Δ (octahedral distortion) – <Cu–ϕ,Cl> relationships to zero distortion. These bond lengths, together with the Cu–Cl bond lengths for (4 + 2)-distorted $Cu^{2+}Cl_6$ octahedra, allow the identification and classification of distortion geometries in mixed-ligand $Cu^{2+}\Phi_6$ octahedra.

$Cu^{2+}\Phi_6$ *with* $\Phi = 4(O^{2-}, OH^-, H_2O) + 2$ Cl

The most common mixed-ligand $Cu^{2+}\Phi_6$ octahedral arrangement in Cu^{2+} oxysalt minerals involves $\Phi = 4(O^{2-}, OH^-, H_2O) + 2$ Cl; minerals containing such octahedra are listed in Table 2. Comparison of these geometries with (4 + 2)-distorted $Cu^{2+}Cl_6$ octahedra (Table 1), (4 + 2)-distorted $Cu^{2+}\phi_6$ octahedra, and undistorted octahedron bond-lengths derived from sums of ionic radii, shows that each of these mixed-ligand octahedra is (4 + 2)-distorted. In each case, the equatorial positions are occupied by the 4(O^{2-}, OH^-, H_2O) ligands, and the two Cl ligands occur at the apical positions (Table 2). As was the case with $Cu^{2+}\phi_6$ octahedra, these mixed-ligand octahedra show considerable variability in distortion, particularly in the apical Cu–Cl bond lengths, which range from 2.55 to 3.21 Å. Variation of the equatorial Cu – (O^{2-}, OH^-, H_2O) distances is more restricted, with an observed range of 1.90 to 2.11 Å. The lower limit of the apical Cu–Cl bond lengths (2.55 Å in nabokoite, Table 2) is close to the expected Cu–Cl undistorted octahedron bond-length (2.43 Å). However, the equatorial octahedron Cu–Φ bond lengths in nabokoite (1.971 Å) indicate that the octahedron is (4 + 2)-distorted.

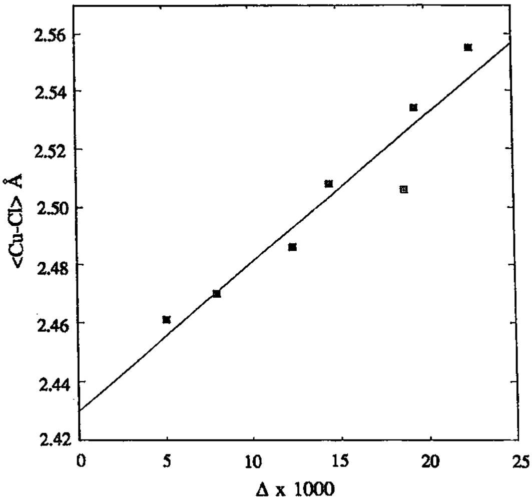

FIG. 2. Mean Cu–Cl bond lengths *versus* octahedral distortion for $Cu^{2+}Cl_6$ octahedra in various inorganic compounds. The least-squares line intercept is at <Cu–Cl> = 2.43 Å.

TABLE 2. MIXED-LIGAND $Cu^{2+}\Phi_6$ OCTAHEDRA IN Cu^{2+} OXYSALT MINERALS WITH $\Phi = 4(O^{2-}, OH^-, H_2O) + 2$ Cl

Mineral	Site	O^{2-}, OH^-, H_2O (Å)				Cl (Å)		Ref.
Cumengéite	Cu(1)	1.99	1.96	1.95	1.95	2.993	2.855	1
	Cu(2)	1.96	1.96	1.96	1.96	2.75	2.75	
Botallackite	Cu(2)	1.920	1.920	2.001	2.001	2.789	2.789	2
Atacamite	Cu(1)	1.940	1.940	2.017	2.017	2.776	2.776	3
Chloroxiphite	Cu	1.98	1.98	1.99	1.99	2.97	2.97	4
Bandylite	Cu	1.98	1.98	1.98	1.98	2.80	2.80	5
Diaboleite	Cu	2.05	2.05	2.05	2.05	2.55	2.95	6
Nabokoite	Cu(2)	1.971	1.971	1.971	1.971	2.553	2.553	7
Francisite	Cu(1)	1.917	1.917	1.96	1.96	3.078	3.078	8
	Cu(2)	1.96	1.96	1.98	1.98	3.206	3.206	
Boleite	Cu	1.90	1.90	2.11	2.11	2.85	2.91	9
Paratacamite	Cu(3)	1.93	1.97	1.98	2.00	2.770	2.818	10
	Cu(4)	1.93	1.99	1.99	2.07	2.753	2.778	
Buttgenbachite	Cu(2)	1.949	1.949	1.974	1.974	2.968	2.968	11
Claringbullite	Cu(1)	1.951	1.951	1.951	1.951	2.997	2.997	12

References: 1: Hawthorne & Groat (1986); 2: Hawthorne (1985); 3: Parise & Hyde (1986); 4: Finney *et al.* (1977); 5: Collin (1951); 6: Rouse (1971); 7: Pertlik & Zemann (1988); 8: Pring *et al.* (1990); 9: Rouse (1973); 10: Fleet (1975); 11: Fanfani *et al.* (1973); 12: Burns *et al.* (1995).

TABLE 3. MIXED-LIGAND $Cu^{2+}\Phi_6$ OCTAHEDRA IN Cu^{2+} OXYSALT MINERALS WITH $\Phi = 5(O^{2-}, OH^-, H_2O) + Cl$

Mineral	Site	O^{2-}, OH^-, H_2O (Å)					Cl (Å)	Ref.
Atacamite	Cu(2)	1.993	1.993	2.010	2.020	2.358	2.750	1
Botallackite	Cu(1)	1.995	1.995	1.998	1.998	2.367	2.732	2
Spangolite	Cu	1.935	1.958	1.979	1.979	2.425	2.835	3
Kamchatkite	Cu(1)	1.928	1.929	2.080	2.37	2.31	2.388	4
	Cu(2)	1.921	1.940	2.069	2.35	2.36	2.401	
Nabokoite	Cu(1)	1.935	1.988	1.998	2.002	2.200	2.769	5
Buttgenbachite	Cu(4)	1.963	1.963	1.983	1.983	2.912	2.801	6

References: 1: Parise & Hyde (1986); 2: Hawthorne (1985); 3: Hawthorne *et al.* (1993); 4: Varaksina *et al.* (1990); 5: Pertlik & Zemann (1988); 6: Fanfani *et al.* (1973).

TABLE 4. MIXED-LIGAND $Cu^{2+}\Phi_6$ OCTAHEDRA IN Cu^{2+} OXYSALT MINERALS WITH $\Phi = 2(O^{2-}, OH^-, H_2O) + 4\ Cl$

Mineral	Site	O^{2-}, OH^-, H_2O (Å)		Cl (Å)				Ref.
Eriochalcite	Cu	1.925	1.925	2.275	2.275	2.938	2.938	1
Chlorothionite	Cu	2.019	2.001	2.252	2.237	3.047	3.047	2

References: 1: Engberg (1970); 2: Giacovazzo *et al.* (1976).

$Cu^{2+}\Phi_6$ *with* $\Phi = 5(O^{2-}, OH^-, H_2O) + 1\ Cl$

Six Cu^{2+} oxysalt minerals contain $Cu^{2+}\Phi_6$ octahedra with $\Phi = 5(O^{2-}, OH^-, H_2O) + 1$ Cl; these are listed in Table 3. Based on comparison with bonds lengths in (4 + 2)-distorted $Cu^{2+}Cl_6$ octahedra (Table 1), (4 + 2)-distorted $Cu^{2+}\phi_6$ octahedra, and undistorted Cu–Φ octahedron bond lengths derived from sums of ionic radii, the mixed-ligand octahedra in atacamite, botallackite, spangolite, buttgenbachite and nabokoite are (4 + 2)-distorted, with the lone Cl in an apical position. These minerals show equatorial Cu – (O^{2-}, OH^-, H_2O) bond-lengths from 1.935 to 1.998 Å, typical values for Cu^{2+} oxysalt minerals. The single apical Cu – (O^{2-}, OH^-, H_2O) bond length ranges from 2.200 to 2.367 Å (excluding the bond length of 2.912 Å in buttgenbachite), values that are long enough to be identified as apical ligands, but that are generally shorter than average Cu–ϕ apical bond-lengths in non-mixed-ligand $Cu^{2+}\phi_6$ octahedra. Apical Cu–Cl bond-lengths range from 2.732 to 2.835 Å in these five minerals, values that are within the range observed in the previous group of mixed-ligand Cu^{2+} oxysalt minerals (see above).

All mixed-ligand $Cu^{2+}\Phi_6$ octahedra with $\Phi = 4(O^{2-}, OH^-, H_2O) + 2$ Cl have the two Cl ligands at apical positions in a (4 + 2)-distorted octahedron (Table 2). Furthermore, five of these six minerals with $\Phi = 5(O^{2-}, OH^-, H_2O) + 1$ Cl have the single Cl located at the apical position of the (4 + 2)-distorted octahedron. However, the two mixed-ligand $Cu^{2+}\Phi_6$ octahedra in kamchatkite (Varaksina *et al.* 1990) do not follow the pattern observed in the rest of the mixed-ligand copper octahedra (Table 3): Here, the single Cl ligands are at equatorial positions in the (4 + 2)-distorted $Cu^{2+}\Phi_6$ octahedra. In both of these octahedra, three equatorial Cu–Φ bonds involve O^{2-}, OH^-, H_2O, with bond lengths from 1.921 to 2.080 Å. The fourth equatorial ligand in each of these octahedra is Cl, with Cu–Cl_{eq} distances of 2.388 and 2.401 Å. Finally, the apical ligands are O^{2-}, OH^-, H_2O, with Cu–Φ_{ap} distances from 2.31 to 2.37 Å, values in the range of Cu–ϕ_{ap} distances in non-mixed-ligand $Cu^{2+}\phi_6$ octahedra.

The Cu(1) and Cu(2) octahedra in kamchatkite each have the two shortest Cu–O equatorial bonds in a *trans* arrangement. The longer Cu–O equatorial bonds [2.080 Å in Cu(1) and 2.069 Å in Cu(2)] are in a *trans* arrangement with the equatorial Cl ligands. Also, the two equatorial Cu–Cl bonds [2.388 Å in Cu(1) and 2.401 Å in Cu(2)] are considerably longer that the average Cu–Cl_{eq} bonds in $Cu^{2+}Cl_6$ octahedra (2.297 Å). These two octahedra may therefore be classified as (2 + 2 + 2)-distorted, and the possibility of dynamic distortion exists; however, anisotropic-displacement parameters are not available for kamchatkite, and so there is no way to assess this possibility.

$Cu^{2+}\Phi_6$ *with* $\Phi = 2(O^{2-}, OH^-, H_2O) + 4\ Cl$

Two Cu^{2+} oxysalt minerals contain $Cu^{2+}\Phi_6$ octahedra with $\Phi = (O^{2-}, OH^-, H_2O) + 4$ Cl: eriochalcite and chlorothionite both contain (4 + 2)-distorted $Cu^{2+}\Phi_6$ octahedra (Table 4). In each case, the $2(O^{2-}, OH^-, H_2O)$ ligands are in a *trans* arrangement in the equatorial positions of the distorted octahedra; the remaining equatorial positions, as well as the apical positions, are occupied by Cl. Equatorial Cu-(O^{2-}, OH^-, H_2O) and Cu–Cl distances are in the ranges observed in other mixed-ligand octahedra, as are the apical Cu–Cl bond lengths (Table 4).

AB INITIO MOLECULAR-ORBITAL STUDIES OF $Cu^{2+}\Phi_6$ MIXED-LIGAND OCTAHEDRA

Molecular-orbital (MO) calculations have been applied to study molecular clusters of varying size as an approximation of local conditions in a crystal structure (*i.e.*, Newton & Gibbs 1980, Gibbs 1982, Lasaga & Gibbs 1987, 1988, 1990, 1991, McCammon *et al.* 1991, Burns & Hawthorne 1995, to mention a few). Recently, Burns & Hawthorne (1995) have applied MO calculations to the study of coordination-geometry structural pathways in Cu^{2+} oxysalt minerals. They found that minimal basis-set calculations for model clusters account for the general features of $Cu^{2+}\phi_n$ polyhedra in minerals. The details of MO calculations as applied in this current study are reviewed by Burns & Hawthorne (1995).

Hartree–Fock MO calculations were done for various clusters and basis-set combinations designed to model $Cu^{2+}\Phi_6$ mixed-ligand octahedra in minerals. The purpose of these calculations is to: (1) determine if Hartree–Fock MO calculations are able to predict the distortion geometries observed for mixed-ligand $Cu^{2+}\Phi_6$ octahedra in minerals, (2) determine the relative energetics of the various possible distortion-geometries of $Cu^{2+}\Phi_6$ octahedra, and (3) calculate potential-energy surfaces for $Cu^{2+}\Phi_6$ octahedra. These surfaces may be used later to derive potential functions for these octahedra, allowing the calculation of crystal structures containing mixed-ligand $Cu^{2+}\Phi_6$ octahedra.

Method of calculation

All calculations were done with Gaussian 86 (Frisch *et al.* 1984) and Gaussian 92 (Frisch *et al.* 1992). The Hartree–Fock calculations are all UHF (spin-unrestricted). Geometries were optimized until the maximum force on any atom did not exceed 0.00045 Hartrees/Bohr and the maximum displacement of any atom in the previous cycle did not exceed 0.0009 Å. The STO–3G* (Hehre *et al.* 1969, Collins *et al.* 1976), 3–21G* (Dobbs & Hehre 1987, Binkley *et al.* 1980, Gordon *et al.* 1982, Pietro *et al.* 1982), STD–SET(1) (Tatewaki & Huzinaga 1979) and DZC–SET(1) (Tatewaki & Huzinaga 1979) basis sets, and the LANL1DZ effective-core-potential basis set (Hay & Wadt 1985a,b, Wadt & Hay 1985) were used in this study.

MO CALCULATIONS FOR $Cu^{2+}\Phi_6$ MIXED-LIGAND OCTAHEDRA WITH $\Phi = 4(O^{2-}, OH^-, H_2O) + 2$ Cl

Several Hartree–Fock calculations were done for clusters designed to model $Cu^{2+}\Phi_6$ with $\Phi = 4(O^{2-}, OH^-, H_2O) + 2$ Cl. As this combination is the most common type of $Cu^{2+}\Phi_6$ mixed-ligand octahedron in minerals, considerable effort was expended in order to find the cluster and basis-set combination that best predicts the geometries of these octahedra.

[$Cu^{2+}(H_2O)_4Cl_2$] cluster

The first calculations were done for the neutral [$Cu^{2+}(H_2O)_4Cl_2$] cluster (Fig. 3). Geometry optimizations for this cluster were done with the constraint that both Cu–Cl apical bond-lengths be equivalent, and that each Cu–(H_2O) equatorial bond-length be equivalent. The H–O–H bond-angles were fixed at 104.5°, and the H–O bond lengths, at 0.957 Å. Optimized geometries (Table 5) were obtained using various basis-set combinations: STO–3G* on all atoms; 3–21G* on all atoms; STD–SET(1) on Cu^{2+} and 3–21G* on all other atoms; DZC–SET(1) on Cu^{2+} and 3–21G* on all the other atoms.

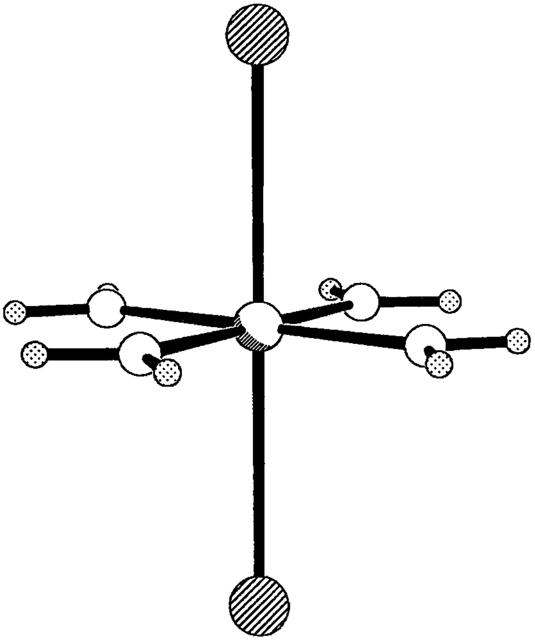

FIG. 3. The [$Cu^{2+}(H_2O)_4Cl_2$] cluster. Cl atoms are shaded with parallel lines, O atoms are open circles, H atoms are stippled, and the Cu atom is shown as an open circle with shading in the lower left corner.

The optimized geometries for the [$Cu^{2+}(H_2O)_4Cl_2$] cluster are compared to $Cu^{2+}\Phi_6$ [$\Phi = 4(O^{2-}, OH^-, H_2O) + 2$Cl] octahedron geometries in minerals in Table 5. With the exception of the calculation done using the 3–21G* basis set on all atoms, all geometries have Cu–Cl distances that are shorter than the range observed in minerals. The STO–3G* basis set performs the poorest in this regard, giving a Cu–Cl distance 0.57 Å shorter than the corresponding average distance observed in minerals. Geometries obtained using the STO–3G* basis set, the STD–SET(1) and 3–21G* basis-set combination, and the DZC–SET(1) and 3–21G* basis-set combination, all have Cu–(H_2O) distances within the range observed in minerals (Table 5). Calculations using the 3–21G* basis set result in a reasonable description of the Cu–Cl bond lengths, but fail to give Cu–(H_2O) distances within the range observed in minerals (Table 5). Thus, *none* of the calculations for the [$Cu^{2+}(H_2O)_4Cl_2$] cluster result in geometries compatible with those observed in mineral structures.

The inadequacy of the [$Cu^{2+}(H_2O)_4Cl_2$] cluster for describing $Cu^{2+}\Phi_6$ mixed-ligand octahedron geometries may be rationalized on the basis of bond strengths. The equatorial ligands are H_2O groups, and the oxygen atoms must contribute about 0.8 valence units to each H atom. This leaves only about 0.4 valence units for the Cu–O bond. However, the apical Cl ligands may contribute up to a full valence unit to the Cu–Cl bond. The calculations for this cluster result in shorter Cu–Cl

TABLE 5. OPTIMIZED GEOMETRIES FOR $Cu^{2+}\Phi_6$ MIXED-LIGAND OCTAHEDRA WITH $\Phi = 4(O^{2-}, OH^-, H_2O) + 2$ Cl

$[Cu^{2+}(H_2O)_4(Cl)_2]$ Cluster			
Basis Set	Cu-O	Cu-Cl	Energy (Hartrees)
STO-3G*	2.055 (Å)	2.287 (Å)	-2831.1590
3-21G*	2.192	2.955	-2848.2710
STD-SET(1) (Cu^{2+}) 3-21G* (Cl^-, O^{2-}, H^+)	2.025	2.516	-2848.0676
DZC-SET(1) (Cu^{2+}) 3-21G* (Cl^-, O^{2-}, H^+)	2.053	2.495	-2848.6847
$[Cu^{2+}(H_2O)_4(ClH)_2]^{2+}$ Cluster			
Basis Set	Cu-O	Cu-Cl	Energy (Hartrees)
STO-3G*	1.951	2.600	-2831.9120
3-21G*	1.895	3.023	-2848.0344
STD-SET(1) (Cu^{2+}) 3-21G* (Cl^-, O^{2-}, H^+)	1.904	2.985	-2848.7160
LANL1DZ	2.023	3.120	
Mineral Data			
	Cu-O	Cu-Cl	
Range	1.90-2.11 (Å)	2.553-3.206 (Å)	
Average	1.978	2.857	
1σ	0.045	0.170	

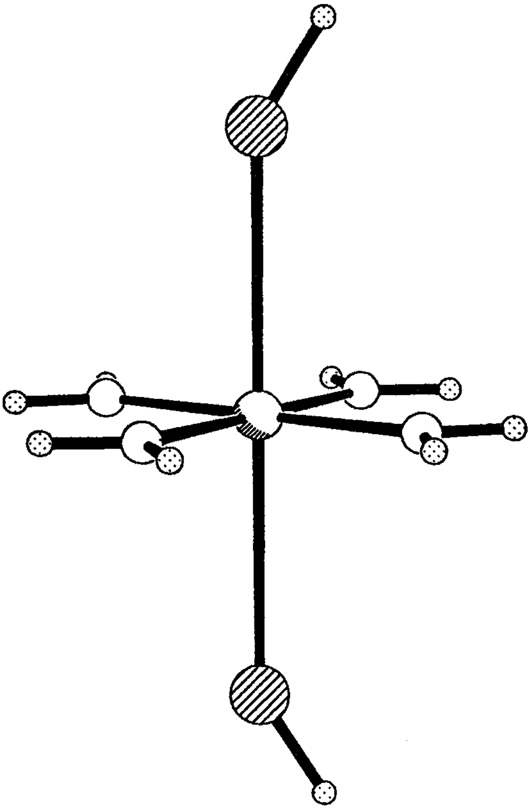

FIG. 4. The $[Cu^{2+}(H_2O)_4(ClH)_2]^{2+}$ cluster. Legend as in Figure 3.

and longer Cu–O distances than expected, in response to the unbalanced bond-strengths associated with each Cu–ligand pair. This inadequacy in the model can, at least partially, be removed by attaching H to the Cl ligands, effectively lowering the valence units associated with the Cu–Cl bonds and simulating interactions that occur when the polyhedron is embedded in the structure.

$[Cu^{2+}(H_2O)_4(ClH)_2]^{2+}$ cluster

Hartree–Fock MO calculations were done for the $[Cu^{2+}(H_2O)_4(ClH)_2]^{2+}$ cluster (Fig. 4). Geometry optimizations were done using the same constraints as for the $[Cu^{2+}(H_2O)_4(Cl)_2]$ cluster, with optimization including the Cl–H bond-lengths and the Cu–Cl–H angles. Optimized geometries (Table 5) were obtained using the following basis-set combinations: STO–3G* on all atoms; 3–21G* on all atoms; STD–SET(1) on Cu^{2+} and 3–21G* on the other atoms; the LANL1DZ effective core potential and valence double-zeta basis set.

. Optimized geometries for the $[Cu^{2+}(H_2O)_4(ClH)_2]^{2+}$ cluster are compared to $Cu^{2+}\Phi_6$ octahedron geometries observed in minerals in Table 5. Each basis-set combination resulted in optimized Cu–O and Cu–Cl bond-lengths that fall within the range observed in minerals. Considerable variability in the calculated bond-lengths was found, with the Cu–O distances ranging from 1.895 Å (3–21G*) to 2.023 Å (LANL1DZ), and Cu–Cl bond lengths from 2.600 Å (STO–3G*) to 3.120 Å (LANL1DZ) (Table 5). The STO–3G* basis-set calculations gave Cu–O bond-lengths that agree with the average Cu–O bond-length in $Cu^{2+}\Phi_6$ [$\Phi = 4(O^{2-}, OH^-, H_2O) + 2Cl$] octahedra in minerals, but the Cu–Cl distance is 0.257 Å shorter than the average observed for minerals. The LANL1DZ basis set resulted in Cu–O and Cu–Cl bond-lengths that are consistently longer than those observed in minerals. The calculations using the 3–21G* basis set on all atoms, and the calculation using the STD–SET(1) basis set on Cu^{2+} with the 3–21G* basis set on the other atoms, led to similar optimized geometries. The calculated Cu–Cl bond-lengths are close to the average observed in $Cu^{2+}\Phi_6$ [$\Phi = 4(O^{2-}, OH^-, H_2O) + 2$ Cl] octahedra in minerals, but the calculated Cu–O distances are somewhat shorter than the average observed in minerals. Based upon the mean absolute deviation of calculated octahedral bond-lengths from the average observed in $Cu^{2+}\Phi_6$ octahedra [Φ = 4(O^{2-}, OH^-, H_2O) + 2Cl] in minerals, we conclude that the combination of the STD–SET(1) basis set on Cu^{2+} and 3–21G* basis set on the rest of the atoms results in the best geometry. Furthermore, the lowest cluster-energy is obtained if this basis-set combination is used.

Each of the optimized geometries obtained using Hartree–Fock calculations for the $[Cu^{2+}(H_2O)_4(ClH)_2]^{2+}$ cluster include Jahn–Teller distortions, as they are all-electron MO calculations. The bond lengths expected for a $Cu^{2+}\Phi_6$ [Φ = 4(O^{2-}, OH^-, H_2O) + 2 Cl] octahedron that is not distorted by a pseudo-Jahn–Teller effect are <Cu^{2+}–(O^{2-}, OH^-, H_2O)> = 2.083 Å (Eby & Hawthorne 1993) and <Cu–Cl> = 2.43 Å (above). Comparison of these bond lengths and those of the optimized clusters (Table 5) shows that all of the optimized cluster geometries are (4 + 2)-distorted octahedra. Searches were conducted for a second energy-minimum, corresponding to a (2 + 4)-distorted octahedron, but none was found.

Potential surface for $[Cu^{2+}(H_2O)_4(ClH)_2]^{2+}$

A potential-energy surface was calculated for the $[Cu^{2+}(H_2O)_4(ClH)_2]^{2+}$ cluster using Hartree–Fock theory and the STD–SET(1) basis set on Cu^{2+} and the 3–21G* basis set on the other atoms (Fig. 5). The potential surface was calculated for a Cu–(H_2O) – Cu–Cl bond-length grid containing 160 points, with Cu–(H_2O) distances ranging from 1.80 to 2.15 Å and Cu–Cl distances ranging from 2.35 to 3.30 Å. Only one energy minimum, corresponding to a (4 + 2)-distorted octahedron, occurs on the potential-energy surface (Fig. 5). The potential has a much stronger curvature parallel to the Cu–(H_2O) equatorial axis than parallel to the apical axis. This is in line with the narrow range of Cu–(O^{2-}, OH^-, H_2O) equatorial bond-lengths compared to the broad range of Cu–Cl apical bond-lengths observed in $Cu^{2+}\Phi_6$ [Φ = 4(O^{2-}, OH^-, H_2O) + 2 Cl] in minerals.

Optimal geometry of the distortion

The calculations for the $[Cu^{2+}(H_2O)_4(ClH)_2]^{2+}$ cluster were done in part to examine the relative stabilities of the distorted octahedra. As already noted, there is no energy-minimum in the potential surface of the (2 + 4)-distorted octahedra, and searches to find such a minimum were unsuccessful. Calculations also were done in search of a minimum corresponding to a (4 + 2)-distorted geometry with H_2O groups in the apical positions, with equatorial positions occupied by two *trans* Cl ligands and two *trans* H_2O ligands. The calculations found no such minimum, and geometry optimization of the trial structures resulted in the same (4 + 2)-distorted octahedra with apical Cl ligands as reported earlier (Table 5).

MO CALCULATIONS FOR $Cu^{2+}\Phi_6$ MIXED-LIGAND OCTAHEDRA WITH Φ = 5(O^{2-}, OH^-, H_2O) + 1 Cl

Hartree–Fock MO calculations were done for the $[Cu^{2+}(H_2O)_5(ClH)]^{2+}$ cluster (Fig. 6) using the STD–SET(1) basis set on Cu^{2+} and the 3–21G* basis set on the other atoms, and also with the 3–21G* basis set on all atoms. These calculations were done to see if the model would give optimized geometries similar to $Cu^{2+}\Phi_6$ [Φ = 5(O^{2-}, OH^-, H_2O) + 1 Cl] octahedra in minerals (Table 3). Geometry optimizations were done with the requirement that all four of the equatorial Cu–(H_2O) bond-lengths be equivalent. The H–O–H angles were fixed at 104.5°, and the H–O

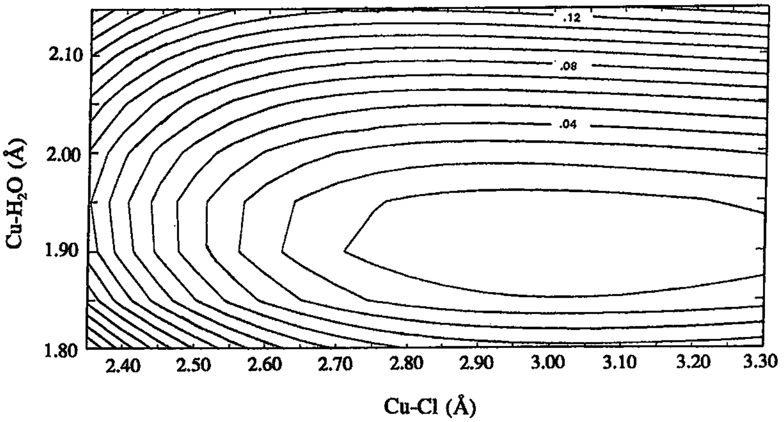

FIG. 5. The potential-energy surface calculated for the $[Cu^{2+}(H_2O)_4(ClH)_2]^{2+}$ cluster using the STD–SET(1) basis set on Cu and the 3–21G* basis set on O, Cl and H. The contour interval is 0.01 Hartrees.

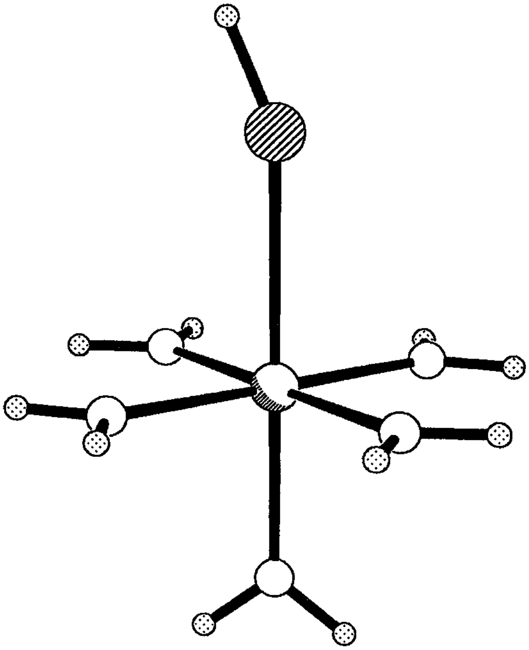

FIG. 6. The $[Cu^{2+}(H_2O)_5(ClH)]^{2+}$ cluster. Legend as in Figure 3.

bond-lengths, at 0.957 Å. The Cl–H bond-length and Cu–Cl–H angle were included in the optimization.

The optimized geometries for the $[Cu^{2+}(H_2O)_5(ClH)]^{2+}$ cluster are compared to the $Cu^{2+}\Phi_6$ [$\Phi = 5(O^{2-}, OH^-, H_2O) + 1\ Cl$] octahedra in minerals in Table 6. Both of these calculations give results that are fairly consistent with observed $Cu^{2+}\Phi_6$ [$\Phi = 5(O^{2-}, OH^-, H_2O) + 1Cl$] geometries in minerals (Table 6). The clusters optimized to become (4 + 2)-distorted octahedra, and the Cl ligand is at the apical position in each case. The optimized $Cu–O_{eq}$ distances fall below the average distance in minerals, but the optimized distances are within that range observed in minerals. The optimized $Cu–O_{ap}$ distances are considerably shorter than the average observed in minerals, and they fall below that range. However, the short $Cu–O_{ap}$ distances predicted by the calculations are in line with the observation that the $Cu–O_{ap}$ distances in $Cu^{2+}\Phi_6$ [$\Phi = 5(O^{2-}, OH^-, H_2O) + 1\ Cl$] octahedra tend to be shorter than those observed in $Cu^{2+}\phi_6$ octahedra. Calculated Cu–Cl bond-lengths are close to, but outside, the range observed in minerals. The optimized Cu–Cl distances obtained using the STD–SET(1) basis set on Cu^{2+} and the 3–21G* basis set on Cl, O^{2-}, H^+ are quite similar to the values observed in minerals. Also, the cluster energy obtained using this basis-set combination is considerably lower than that obtained using the 3–21G* basis set on all atoms (Table 6).

TABLE 6. OPTIMIZED GEOMETRIES FOR $Cu^{2+}\Phi_6$ MIXED-LIGAND OCTAHEDRA WITH $\Phi = 5(O^{2-}, OH^-, H_2O) + 1\ Cl$

$[Cu^{2+}(H_2O)_5(ClH)]^{2+}$				
Basis Set	$Cu\text{-}O_{eq}$(Å)	$Cu\text{-}O_{ap}$(Å)	Cu-Cl (Å)	Energy (Hartrees)
STD-SET(1) (Cu^{2+}) 3-21G* (Cl^-, O^{2-}, H^+)	1.933	2.130	2.851	-2466.0795
3-21G*	1.921	2.117	3.056	-2465.4004
Range in Minerals⁺	1.92-2.20	2.20-2.91	2.732-2.835	
Average⁺	1.982	2.452	2.777	

+ excluding the octahedra in kamchatkite

Optimal geometry of the distorted octahedra

As was the case with the $Cu^{2+}\Phi_6$ [$\Phi = 4(O^{2-}, OH^-, H_2O) + 2\ Cl$] calculations, these calculations indicate that there is no energy minimum corresponding to a (2 + 4)-distorted $Cu^{2+}\Phi_6$ [$\Phi = 5(O^{2-}, OH^-, H_2O) + 1\ Cl$] octahedron. Searches for such a minimum were unsuccessful, and geometry optimization commencing from various starting geometries all resulted in a (4 + 2)-distorted octahedron geometry. Attempts to optimize the geometry for a cluster having the Cl ligand at an equatorial position also were unsuccessful, again resulting in the (4 + 2)-distorted octahedron with the Cl ligand in an apical position.

Potential surface for $[Cu^{2+}(H_2O)_5(ClH)]^{2+}$

A three-dimensional potential-energy surface was calculated for the $[Cu^{2+}(H_2O)_5(ClH)]^{2+}$ cluster using the STD–SET(1) basis set on Cu^{2+} and the 3–21G* basis set on the other atoms. The Hartree–Fock energies were calculated for 520 combinations of $Cu–O_{eq}$, $Cu–O_{ap}$ and Cu–Cl distances. Sections of constant Cu–Cl through the three-dimensional potential are given in Figure 7. The potential-energy minimum is strongly anisotropic, with considerable elongation along the $Cu–O_{ap}$ direction. This elongation is consistent with the range of $Cu–O_{ap}$ bond lengths in $Cu^{2+}\Phi_6$ [$\Phi = 5(O^{2-}, OH^-, H_2O) + 1\ Cl$] octahedra in minerals. The relatively steep potential in the $Cu–O_{eq}$ direction is also consistent with the relatively narrow range of these bond lengths in $Cu^{2+}\Phi_6$ [$\Phi = 5(O^{2-}, OH^-, H_2O) + 1\ Cl$] octahedra in minerals.

CONCLUSIONS

Mixed-ligand $Cu^{2+}\Phi_6$ octahedra in minerals

Consideration of all $Cu^{2+}\Phi_6$ mixed-ligand octahedra in minerals has shown that the octahedra are invariably

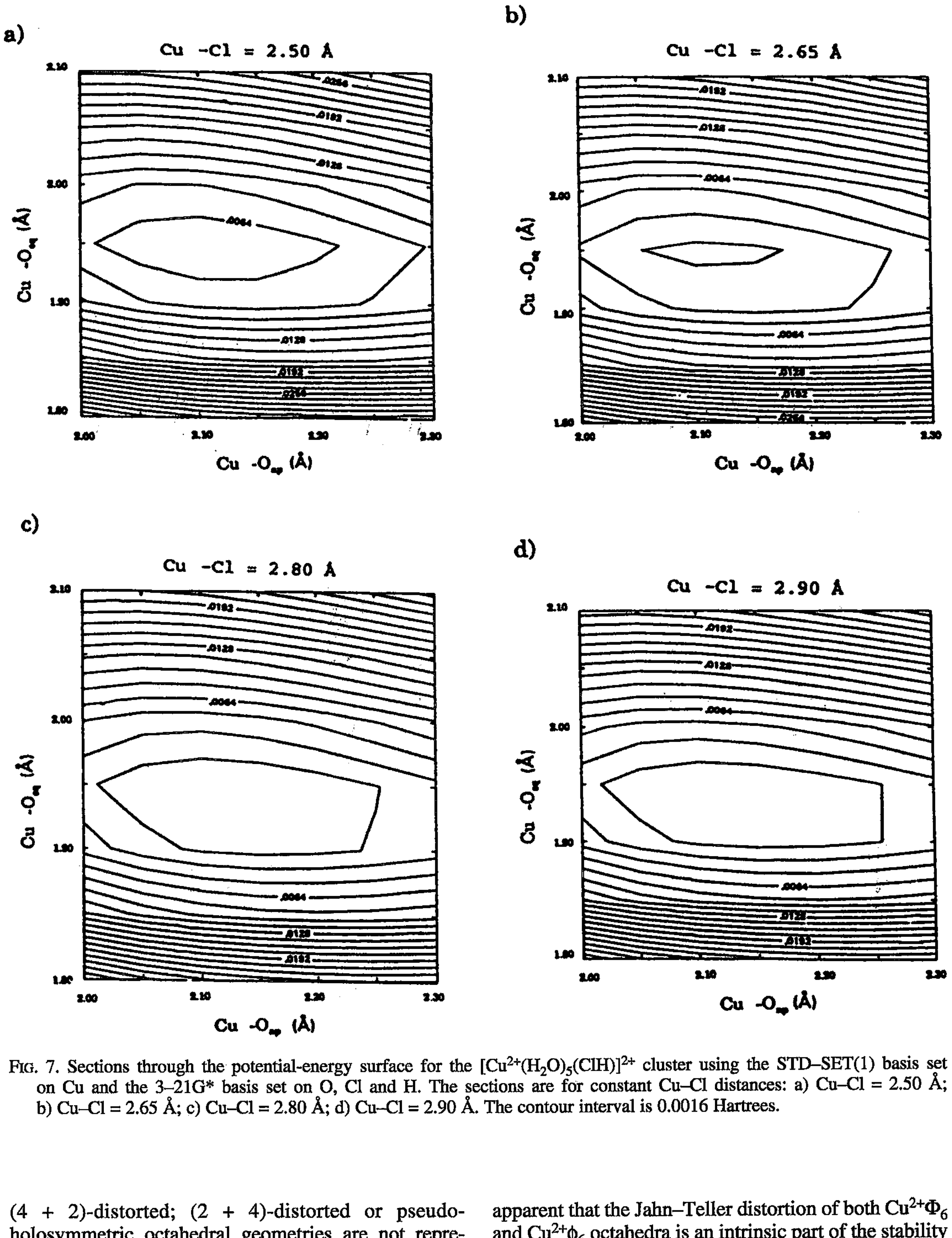

FIG. 7. Sections through the potential-energy surface for the $[Cu^{2+}(H_2O)_5(ClH)]^{2+}$ cluster using the STD–SET(1) basis set on Cu and the 3–21G* basis set on O, Cl and H. The sections are for constant Cu–Cl distances: a) Cu–Cl = 2.50 Å; b) Cu–Cl = 2.65 Å; c) Cu–Cl = 2.80 Å; d) Cu–Cl = 2.90 Å. The contour interval is 0.0016 Hartrees.

(4 + 2)-distorted; (2 + 4)-distorted or pseudo-holosymmetric octahedral geometries are not represented. The complete dominance of (4 + 2)-distortion in mixed-ligand octahedra is consistent with $Cu^{2+}\phi_6$ ($\phi = O^{2-}$, OH^-, H_2O) octahedra in minerals, which are also almost invariably (4 + 2)-distorted. It is now apparent that the Jahn–Teller distortion of both $Cu^{2+}\Phi_6$ and $Cu^{2+}\phi_6$ octahedra is an intrinsic part of the stability of minerals containing such octahedra; the structural connectivity must be capable of accommodating such a distortion if the structure is to be stable.

Mixed-ligand $Cu^{2+}\Phi_6$ octahedra with 1, 2 or 4 Cl ligands occur in minerals, and those containing 2 Cl ligands are the most common. Notably, $Cu^{2+}\Phi_6$ octahedra with 3 or 5 Cl ligands do not occur in mineral structures. Molecular-orbital calculations for such octahedra have not yet been done, and the current work does not provide an explanation for the absence of such octahedra in minerals. Presumably, this absence is attributable either to the fairly small sample-size, or to the fact that such octahedra are energetically unfavorable compared to alternative arrangements.

There are numerous examples of mixed-ligand $Cu^{2+}\Phi_6$ octahedra in minerals. For such octahedra containing 2 Cl ligands, both Cl ligands are always located at the apical positions of (4 + 2)-distorted octahedra. Likewise, with the possible exception of one mineral (kamchatkite, for which further work is suggested), all mixed-ligand octahedra containing 1 Cl have that Cl ligand at one of the two apical positions of the (4 + 2)-distorted octahedron. The trend is continued in octahedra with 4 Cl; 2 Cl ligands occur at the apical positions of (4 + 2)-distorted octahedra.

Molecular-orbital calculations

Various Hartree–Fock MO calculations for model mixed-ligand $Cu^{2+}\Phi_6$ clusters have been done. Calculations for the $[Cu^{2+}(H_2O)_4(ClH)_2]^{2+}$ and $[Cu^{2+}(H_2O)_5(ClH)]^{2+}$ clusters, using the STD–SET(1) basis set on Cu^{2+} and the 3–21G* basis set on the other atoms, gave Cu–O and Cu–Cl bond lengths that are in good agreement with the values observed in minerals. Potential-energy surfaces calculated for these clusters are in good qualitative agreement with geometries of $Cu^{2+}\Phi_6$ octahedra in minerals. In addition, all calculations predict that the (4 + 2)-distorted octahedral geometry is the only stable one for mixed-ligand $Cu^{2+}\Phi_6$ octahedra containing 1 or 2 Cl ligands, a result that is in perfect accord with the geometries observed in minerals. The molecular-orbital calculations predict that the Cl ligands in $Cu^{2+}\Phi_6$ octahedra with 1 or 2 Cl will occur in the apical positions of the (4 + 2)-distorted octahedron, again in excellent agreement with geometries in minerals. These results show that molecular-orbital calculations using the cluster approach are a very effective way to model local effects in Cu^{2+} oxysalt structures.

ACKNOWLEDGEMENTS

This work was supported by the Natural Sciences and Engineering Research Council of Canada in the form of a Post-Graduate Fellowship to PCB and Operating and Equipment Grants to FCH. The University of Manitoba provided some of the computer resources used in this study. The manuscript was improved following the comments of two anonymous referees and editorial work by Drs. R.C. Rouse and R.F. Martin.

REFERENCES

BINKLEY, J.S., POPLE, J.A. & HEHRE, W.J. (1980): Self-consistent molecular orbital methods. 21. Small split-valence basis sets for first-row elements. *J. Am. Chem. Soc.* **102**, 939-947.

BURDETT, J.K. (1980): *Molecular Shapes.* Wiley, New York, N.Y.

________ & EISENSTEIN, O. (1992): From three- to four-coordination in copper (I) and silver (I). *Inorg. Chem.* **31**, 1758-1762.

BURNS, P.C. (1994): *The Stereochemistry of Cu^{2+} Oxysalt Minerals: an ab initio Molecular-Orbital Approach.* Ph.D. thesis, Univ. of Manitoba, Winnipeg, Manitoba.

________, COOPER, M.A. & HAWTHORNE, F.C. (1995): Claringbullite: a Cu^{2+} oxysalt with Cu^{2+} in trigonal-prismatic coordination. *Can. Mineral.* **33**, 633-639.

________ & HAWTHORNE, F.C. (1993): Tolbachite, $CuCl_2$, the first example of Cu^{2+} octahedrally coordinated by Cl^-. *Am. Mineral.* **78**, 187-189.

________ & ________ (1995): Coordination-geometry structural pathways in Cu^{2+} oxysalt minerals. *Can. Mineral.* **33**, 889-905.

COLLIN, R.L. (1951): The crystal structure of bandylite, $CuCl_2{\cdot}CuB_2O_4{\cdot}4H_2O$. *Acta Crystallogr.* **4**, 204-209.

COLLINS, J.B., SCHLEYER, P.V.R., BINKLEY, J.S. & POPLE, J.A. (1976): Self-consistent molecular orbital methods. XVII. Geometries and binding energies of second-row molecules. A comparison of three basis sets. *J. Chem. Phys.* **64**, 5142-5151.

CRAMA, W.J. (1981a): The cooperative Jahn–Teller distorted structure of $RbCuCl_3$. *J. Solid State Chem.* **39**, 168-172.

________ (1981b): Structures of trirubidium heptachlorodicuprate (II). *Acta Crystallogr.* **B37**, 662-664.

DEETH, R.J. & HITCHMAN, M.A. (1986): Factors influencing Jahn–Teller distortions of six-coordinate copper (II) and low-spin nickel (II) complexes. *Inorg. Chem.* **25**, 1225-1233.

DOBBS, K.D. & HEHRE, W.J. (1987): Molecular orbital theory of the properties of inorganic and organometallic compounds. 5. Extended basis sets for first-row transition metals. *J. Comp. Chem.* **8**(6), 861-879.

EBY, R.K. & HAWTHORNE, F.C. (1993): Structural relations in copper oxysalt minerals. I. Structural hierarchy. *Acta Crystallogr.* **B49**, 28-56.

ENGBERG, A. (1970): An X-ray refinement of the crystal structure of copper (II) chloride dihydrate. *Acta Chemica Scandinavica* **24**, 3510-3526.

FANFANI, L., NUNZI, A., ZANAZZI, P.F. & ZANZARI, A.R. (1973): The crystal structure of buttgenbachite. *Mineral. Mag.* **39**, 264-270.

FINNEY, J.J., GRAEBER, E.J., ROSENWEIG, A. & HAMILTON, R.D. (1977): The structure of chloroxiphite, $Pb_3CuO_2(OH)_2Cl_2$. *Mineral. Mag.* **41**, 357-361.

FLEET, M.E. (1975): The crystal structure of paratacamite, $Cu_2(OH)_3Cl$. *Acta Crystallogr.* **B31**, 183-187.

FRISCH, M.J., BINKLEY, J.S., SCHLEGEL, H.B., RAGHAVACHARI, K., MELIUS, C.F., MARTIN, R.L., STEWART, J.J.P., BOBROWICZ, F.W., ROHLFING, C.M., LAHN, L.R., DEFREES, D.J., SEEGER, R., WHITESIDE, R.A., FOX, D.J., FLEUDER, E.M. & POPLE, J.A. (1984): *Gaussian 86.* Carnegie-Mellon Quantum Chemistry Publishing Unit, Pittsburgh, Pennsylvania.

________, TRUCKS, G.W., HEAD-GORDON, M., GILL, P.M.W., WONG, M.W., FORESMAN, J.B., JOHNSON, B.G., SCHLEGEL, H.B., ROBB, M.A., REPLOGLE, E.S., GOMPERTS, R., ANDRES, J.L., RAGHAVACHARI, K., BINKLEY, J.S., GONZALEZ, C., MARTIN, R.L., FOX, D.J., DEFREES, D.J., BAKER, J., STEWART, J.J.P. & POPLE, J.A. (1992): *Gaussian 92, Revision C.* Gaussian Inc., Pittsburgh, Pennsylvania.

GIACOVAZZO, C., SCANDALE, E. & SCORDARI, F. (1976): The crystal structure of chlorotionite, $CuK_2Cl_2SO_4$. *Z. Kristallogr.* **144**, 226-237.

GIBBS, G.V. (1982): Molecules as models for bonding in silicates. *Am. Mineral.* **67**, 421-450.

GORDON, M.S., BINKLEY, J.S., POPLE, J.A., PIETRO, W.J. & HEHRE, W.J. (1982): Self consistent molecular-orbital methods. 22. Small split-valence basis sets for second-row elements. *J. Am. Chem. Soc.* **104**, 2797-2803.

HAWTHORNE, F.C. (1985): Refinement of the crystal structure of botallackite. *Mineral. Mag.* **49**, 87-89.

________ & GROAT, L.A. (1986): The crystal structure and chemical composition of cumengéite. *Mineral. Mag.* **50**, 157-162.

________, KIMATA, M. & EBY, R.K. (1993): The crystal structure of spangolite, a complex copper sulfate sheet mineral. *Am. Mineral.* **78**, 649-652.

HAY, J.P. & WADT, W.R. (1985a): *Ab initio* effective core potentials for molecular calculations. Potentials for the transition metal atoms Sc to Hg. *J. Chem. Phys.* **82**, 270-283.

________ & ________ (1985b): *Ab initio* effective core potentials for molecular calculations. Potentials for K to Au including the outermost core orbitals. *J. Chem. Phys.* **82**, 299-310.

HEHRE, W.J., STEWART, R.F. & POPLE, J.A. (1969): Self-consistent molecular-orbital methods. I. Use of gaussian expansions of slater-type atomic orbitals. *J. Chem. Phys.* **51**, 2657-2664.

JAHN, H.A. & TELLER, E. (1937): Stability of polyatomic molecules in degenerate electronic states. I. Orbital degeneracy. *Proc. Roy. Soc.* **A161**, 220-235.

LASAGA, A.C. & GIBBS, G.V. (1987): Applications of quantum mechanical potential surfaces to mineral physics calculations. *Phys. Chem. Minerals* **14**, 107-117.

________ & ________ (1988): Quantum mechanical potential surfaces and calculations on minerals and molecular clusters. I. STO–3G and 6–31G* results. *Phys. Chem. Minerals* **16**, 29-41.

________ & ________ (1990): *Ab initio* quantum mechanical calculations of water–rock interactions: adsorption and hydrolysis reactions. *Am. J. Sci.* **290**, 263-295.

________ & ________ (1991): Quantum mechanical Hartree–Fock potential surfaces and calculations on minerals. *Phys. Chem. Minerals* **17**, 485-491.

MCCAMMON, C.A., BROWN, T.H. & MEAGHER, E.P. (1991): Calculation of the equation of state and elastic moduli of MgO using molecular orbital theory. *Phys. Chem. Minerals* **17**, 622-628.

NEWTON, M.D. & GIBBS, G.V. (1980): *Ab initio* calculated geometries and charge distributions for H_4SiO_4 and $H_6Si_2O_7$ compared with experimental values for silicates and siloxanes. *Phys. Chem. Minerals* **6**, 221-246.

ORGEL, L.E. (1966): *An Introduction to Transition Metal Chemistry: Ligand Field Theory* (2nd ed.). Methuen, London, U.K.

PARISE, J.B. & HYDE, B.G. (1986): The structure of atacamite and its relationship to spinel. *Acta Crystallogr.* **C42**, 1277-1280.

PERTLIK, F. & ZEMANN, J. (1988): The crystal structure of nabokoite, $Cu_7TeO_4(SO_4)_5{\cdot}KCl$: the first example of a Te(IV)O_4 pyramid with exactly tetragonal symmetry. *Mineral. Petrol.* **38**, 291-298.

PIETRO, W.J., FRANCI, W.H., HEHRE, W.J., DEFREES, D.J., POPLE, J.A. & BINKLEY, J.S. (1982): Self-consistent molecular orbital methods. 24. Supplemented small split-valence basis sets for second row elements. *J. Am. Chem. Soc.* **104**, 5039-5048.

PRING, A., GATEHOUSE, B.M. & BIRCH, W.D. (1990): Francisite, $Cu_3Bi(SeO_3)_2O_2Cl$, a new mineral from Iron Monarch, South Australia: description and crystal structure. *Am. Mineral.* **75**, 1421-1425.

ROUSE, R.C. (1971): The crystal chemistry of diaboleite. *Z. Kristallogr.* **134**, 69-80.

________ (1973): The crystal structure of boleite – a mineral containing silver atom clusters. *J. Solid State Chem.* **6**, 86-92.

SCHÄFER, V.H., BINNEWIES, M., LAUMANNS, R. & WÄCHTER, H. (1980): $CuAl_2Cl_8$. Darstellung und Kristallstruktur. *Z. Anorg. Allg. Chem.* **461**, 31-34.

SCHLUETER, A.W., JACOBSON, R.A. & RUNDLE, R.E. (1966): A redetermination of the crystal structure of $CsCuCl_3$. *Inorg. Chem.* **5**, 277-280.

SHANNON, R.D. (1976): Revised effective ionic radii and systematic studies of interatomic distances in halides and chalcogenides. *Acta Crystallogr.* **A32**, 751-767.

TATEWAKI, H. & HUZINAGA, S. (1979): A systematic preparation of new contracted Gaussian-type orbital set. I. Transition metal atoms from Sc to Zn. *J. Chem. Phys.* **71**, 4339-4348.

VARAKSINA, T.V., FUNDAMENSKY, V.S., FILATOV, S.K. & VERGASOVA, L.P. (1990): The crystal structure of kamchatkite, a new naturally occurring oxychloride sulphate of potassium and copper. *Mineral. Mag.* **54**, 613-616.

WADT, W.R. & HAY, J.P. (1985): *Ab initio* effective core potentials for molecular calculations. Potentials for main group elements Na to Bi. *J. Chem. Phys.* **82**, 284-298.

WHITTAKER, E.J.W. & MUNTUS, R. (1970): Ionic radii for use in geochemistry. *Geochim. Cosmochim. Acta* **34**, 945-956.

WILLETT, R.D., DWIGGINS, C., JR., KRUH, R.F. & RUNDLE, R.E. (1963): Crystal structures of $KCuCl_3$ and NH_4CuCl_3. *J. Chem. Phys.* **38**, 2429-2436.

Received October 18, 1994, revised manuscript accepted August 8, 1995.